

1      **Snowball Earths, population bottlenecks, and *Prochlorococcus* evolution**

2      Hao Zhang<sup>1^\*</sup>, Ying Sun<sup>1^\*</sup>, Qinglu Zeng<sup>2</sup>, Sean A. Crowe<sup>3</sup>, Haiwei Luo<sup>1\*</sup>

3

4      <sup>1</sup>Simon F. S. Li Marine Science Laboratory, School of Life Sciences and State Key Laboratory  
5      of Agrobiotechnology, The Chinese University of Hong Kong, Shatin, Hong Kong SAR

6      <sup>2</sup>Department of Ocean Science, The Hong Kong University of Science and Technology, Clear  
7      Water Bay, Hong Kong SAR

8      <sup>3</sup>Department of Earth Sciences, School of Biological Sciences, and Swire Institute for Marine  
9      Science (SWIMS), University of Hong Kong, Pokfulam Road, Hong Kong SAR

10     ^These authors contributed equally to this study.

11

12     **\*Corresponding author:** Haiwei Luo

13     **Email:** hluo2006@gmail.com

14     **Competing Interest Statement:** The authors declare no competing interests.

15     **Keywords:** *Prochlorococcus*, Neoproterozoic Snowball Earth, genome reduction, molecular  
16     dating.

17     **Abstract**

18           *Prochlorococcus* are the most abundant photosynthetic organisms in the modern ocean. A  
19           massive DNA loss event occurred in their early evolutionary history, leading to highly reduced  
20           genomes in nearly all lineages, as well as enhanced efficiency in both nutrient uptake and light  
21           absorption. The environmental landscape that shaped this ancient genome reduction, however,  
22           remained unknown. Through careful molecular clock analyses, we established that this  
23           *Prochlorococcus* genome reduction occurred during the Neoproterozoic Snowball Earth climate  
24           catastrophe. The lethally low temperature and exceedingly dim light during the Snowball Earth  
25           event would have inhibited *Prochlorococcus* growth and proliferation and caused severe  
26           population bottlenecks. These bottlenecks are recorded as an excess of deleterious mutations that  
27           accumulated across genomic regions in the descendant lineages. *Prochlorococcus* adaptation to  
28           extreme environmental conditions during Snowball Earth intervals can be inferred by tracing the  
29           evolutionary paths of genes that encode key metabolic potential. This metabolic potential  
30           includes modified lipopolysaccharide structure, strengthened peptidoglycan biosynthesis, the  
31           replacement of a sophisticated circadian clock with an hourglass-like mechanism that resets daily  
32           for dim light adaption, and the adoption of ammonia diffusion as an efficient membrane  
33           transporter-independent mode of nitrogen acquisition. In this way, the Neoproterozoic Snowball  
34           Earth event altered the physiological characters of *Prochlorococcus*, shaping their ecologically  
35           vital role as the most abundant primary producers in the modern oceans.

## 36      **Introduction**

37      *Prochlorococcus* are the smallest and most abundant photosynthetic organisms on Earth (1).  
38      They are prevalent throughout the photic zone of the oligotrophic oceans between 40 °N and  
39      40 °S (1), where they account for more than 40% of the biomass and contribute almost half of the  
40      net primary production (2). *Prochlorococcus* have diversified into two major phylogenetic  
41      groups with distinct ecology (ecotypes), with the high-light (HL) adapted monophyletic group  
42      imbedded in the low-light (LL) adapted paraphyletic group (3). The distinct ecotypes of  
43      *Prochlorococcus* evolved different pigments, light-harvesting systems, and phycobiliproteins,  
44      which allowed for efficient light absorption in the water column (4), and thus increased growth  
45      rates and primary production (5).

46      *Prochlorococcus* genomes have been shaped by stepwise streamlining, including a major  
47      genome reduction in their early evolution and a few minor modifications that followed (6, 7).  
48      Modern marine *Prochlorococcus* lineages, in particular those with small genomes, show very  
49      low ratios of nonsynonymous ( $d_N$ ) to synonymous ( $d_S$ ) nucleotide substitution rates, suggesting  
50      that natural selection is a highly efficient throttle on the accumulation of deleterious mutations  
51      (i.e., nonsynonymous mutations) in *Prochlorococcus* (6, 8). On long time scales, however,  
52      nucleotide substitutions at synonymous sites become saturated, invalidating the use of  $d_N/d_S$  to  
53      infer selection efficiency in deep time (9). Thus, an alternative approach focuses instead on  
54      different types of nonsynonymous substitutions leading to radical versus conservative changes in  
55      amino acid sequences, with the former more likely to be deleterious (10, 11). Excess radical  
56      mutations accumulate from random fixations of deleterious mutations by genetic drift (i.e.,  
57      reduced efficiency of selection). Using this approach reveals that the major genome reduction in

58 *Prochlorococcus* took place under reduced selection efficiency (9) and implies that the ancient  
59 population went through severe bottlenecks as the likely result of environmental catastrophe.

60 The environmental context underlying *Prochlorococcus* genome reduction remains  
61 unknown, however, and precise molecular dating is needed to link this important evolutionary  
62 event to its possible environmental drivers. By implementing comprehensive molecular clock  
63 analyses, we now link the early major genome reduction event of *Prochlorococcus* to the  
64 Neoproterozoic Snowball Earth events. These catastrophic disruptions to the Earth system would  
65 likely have challenged warm-water-loving photosynthetic *Prochlorococcus*, with strong potential  
66 to cause the population bottlenecks inferred from the genome sequences described above.

67 *Prochlorococcus* survived this catastrophe through likely gains and losses of key metabolic  
68 functions reconstructed from the same genome sequences, which have a far-reaching impact on  
69 their success in today's oceans. *Prochlorococcus* are thus vital "guardians of metabolism" (12),  
70 shepherding genes critical to the functioning of the biosphere across environmental catastrophes,  
71 including global glaciations.

72

### 73 **Results and Discussion**

74 *Prochlorococcus* experienced a massive gene loss event on the ancestral branch leading to  
75 the last common ancestor (LCA) of clades HL, LLI, and LLII/III (6, 7, 13). This is confirmed by  
76 our analysis, which reconstructed 366 and 107 gene family losses and gains on this branch,  
77 respectively (Fig. 1A & S1). On the same ancestral branch, it was shown that  $d_R/d_C$  is  
78 significantly elevated compared to the sister ancestral branch leading to the LCA of the LLIV  
79 (9), which was validated here (both sign test and paired *t*-test,  $p < 0.001$ ; Fig. 1B). These results  
80 confirm that the major genome reduction event occurring on this branch was likely driven by

81 genetic drift as a result of one or recurrent population bottlenecks (9). Given the global  
82 distribution and abundance of *Prochlorococcus*, and cyanobacteria more generally, such a  
83 bottleneck would likely require a global-scale event, like an environmental or climate catastrophe  
84 (e.g. meteorite impact, large igneous province emplacement, or glaciation).

85 To establish the environmental context for the large, ancient genome reduction, we estimated  
86 the timeline of *Prochlorococcus* evolution by implementing molecular clock analyses based on  
87 essential calibrations available in the cyanobacterial lineage. We recognize that the use of  
88 calibration sets adapted from previous studies (under calibrations C1-C8 in Table S1 with related  
89 references included there) results in up to ~320 Ma disparity (Fig. S2A) in the estimated time for  
90 the LCA of *Prochlorococcus* HL, LLI and LLII/III clades that emerged with the major genome  
91 reduction. We note that the calibrations in previous studies were not properly used. For example,  
92 the akinete fossil identified to 2,100 Mya was used as either the maximum bound or the  
93 minimum bound to calibrate the crown group of Nostocales (14, 15). However, given the fact  
94 that apomorphic character must evolve earlier than the divergence of crown group,  
95 morphological fossils can only serve as the minimum bounds on total groups of assigned  
96 lineages (16) (see Section 2.3 in Supplemental Methods for details). Thus, in the present study,  
97 we modified the calibration sets by constraining the lower bounds of the Nostocales (and the  
98 Pleurocapsales) total groups with morphological fossils and by leaving their upper bounds open  
99 (C9-C14; Table S1). Intriguingly, the variation is reduced to less than 10 Ma when these  
100 modified calibration sets are used (Fig. S2A).

101 Recent identification of non-oxygenic Cyanobacteria lineages such as Melainabacteria and  
102 Sericytochromatia as sister groups of oxygenic Cyanobacteria (17, 18) provides an alternative  
103 way to constrain the evolution of oxygenic Cyanobacteria. Specifically, given that oxygenic

104 photosynthesis evolved at the stem lineage of oxygenic Cyanobacteria, we constrained the  
105 minimum age of the total Cyanobacteria group at 3.0 Ga, which is supported by geochemical  
106 evidence as the time when atmospheric oxygen became available (19, 20). To avoid the overly  
107 precise and potentially misleading age estimates, we calibrated the upper limit of the  
108 Cyanobacteria root using the ages when the planet Earth formed and became habitable (C15-C38  
109 in Table S1; see Section 2.3 in Supplemental Methods for details). Using this strategy, we show  
110 that the age of *Prochlorococcus* major genome reduction remains stable when non-oxygenic  
111 Cyanobacteria outgroups were included (Fig. S2B). Since including the non-oxygenic  
112 Cyanobacteria have consistently reduced the precision of posterior age estimates, manifested as  
113 the higher slopes of the regression line between highest posterior density (HPD) width and the  
114 posterior age estimates compared to those without including these lineages (C15-C38 versus C1-  
115 C14 in Fig. S3; also see Section 2.6 in Supplemental Methods for an extended discussion), we  
116 focus on the crown oxygenic Cyanobacteria group dating (C7-C14) in the following discussions.

117 By comparing the width of the 95% HPD derived from each molecular clock analysis (Fig.  
118 S3), we inferred the most precise timeline of *Prochlorococcus* evolution (corresponding to the  
119 calibration set C14 in Table S1; see Section 2.3 in Supplemental Methods). Our time estimates  
120 revealed that the LCA of *Prochlorococcus* HL, LLI, and LLII/III clades diversified at 682 Mya  
121 (95% HPD 632-732 Mya), precisely dating the genome reduction event to this time. A 682 Mya  
122 date for the emergence of the LCA of *Prochlorococcus* HL, LLI, and LLII/III clades places the  
123 large genome reduction that took place in this lineage firmly within the Cryogenian Period (~720  
124 to 635 Mya; Fig. 1A) and implicates the Snowball Earth icehouse climate conditions eponymous  
125 with the Period in the corresponding *Prochlorococcus* population bottleneck. We, therefore, refer  
126 to this ancestor as SBE-LCA (see Fig. 1A), short for “Snowball Earth” LCA. The

127 Neoproterozoic climate catastrophe culminated in the Sturtian (~717 to 659 Mya) and Marinoan  
128 (~645 to 635 Mya) glaciations (Fig. 1A), which stretched from the poles to sea level near the  
129 equators, possibly wrapping the entire Earth under a frozen skin (21). This “Snowball Earth”  
130 persisted with the freezing temperature of seawater below the ice sheet lowered to -3.5°C (22).  
131 Since all assayed *Prochlorococcus* strains, including those affiliated with the basal LL ecotypes,  
132 reach maximum growth rates at approximately 25°C and rarely survive when the temperature  
133 drops to ~10°C (Fig. 1C) (23), we propose that extreme climate cooling during the  
134 Neoproterozoic Snowball Earth events was likely the major driver of severe bottlenecks in early  
135 *Prochlorococcus* populations.

136 Survival of *Prochlorococcus* populations through the Cryogenian would have required  
137 refugia, the nature of which would have shaped continued *Prochlorococcus* evolution. A variety  
138 of biotic refugia have been identified during Snowball Earth intervals, including the sea-ice brine  
139 channels within ice grounding-line crack systems (24) and cryoconite holes/ponds on the surface  
140 of the sublimation zone, which may have represented ~12% of the global sea glacier surface (25)  
141 (Fig. 1D). Despite providing the essential space for *Prochlorococcus* survival, these refugia  
142 would have presented a number of environmental stresses to *Prochlorococcus* populations such  
143 as low temperature, dim light, and limited nutrients (24-26). *Prochlorococcus* thus evolved a  
144 number of adaptive mechanisms to cope with these stresses via gene gains and losses, which we  
145 assessed by reconstructing the evolutionary paths of imprints that the Snowball Earth climate left  
146 in extant *Prochlorococcus* genomes.

147 Among these stresses, the most prominent was likely lethally low temperature. Maintaining  
148 membrane fluidity is of paramount importance under low-temperature conditions, which is  
149 largely achieved by the activities of fatty acid desaturase encoded by *desA* and *desC*. As a result,

150 we inferred that these genes were retained in SBE-LCA (Fig. 1A). Lipopolysaccharide (LPS) in  
151 the outer membrane is known to provide the first line of defense against harsh environments  
152 (27), which contains the O-specific polysaccharide, the glycolipid anchor lipid A, and the  
153 polysaccharide core region. Based on our analyses, genes encoding the polysaccharide core  
154 region (*kdsABCD* for 3-deoxy-d-manno-octulosonate biosynthesis; Fig. 1A) were likely lost at  
155 SBE-LCA, while those encoding the other components were retained (*lpxABCD* and *rfbABC* for  
156 Lipid A precursor and O-specific LPS precursor biosynthesis; Fig. 1A). This inference is  
157 consistent with a previous conclusion that the loss of the LPS core region would increase the  
158 hydrophobicity and permeability of the cell envelope (28) to protect against cold conditions (29).  
159 Another metabolic modification in SBE-LCA was related to heat shock proteins (HSPs), which  
160 play crucial roles in tolerating environmental stresses including thermal shocks. Typically, HSPs  
161 are tightly regulated, as they respond quickly to stress and turn off rapidly once the stress  
162 disappears (30). However, the HSP repressor protein encoded by *hrcA* was inferred to be lost at  
163 SBE-LCA, which thus likely allowed the organism to continuously express HSPs to cope with  
164 prolonged lethally low temperature. In fact, constitutive expression of HSPs occurs in polar  
165 organisms such as the Antarctic ciliate *Euplotes focialis* (31) and the polar insect *Belgica*  
166 *antarctica* larvae (32). Extremely low temperature also made substrate acquisition difficult due  
167 to increased lipid stiffness and decreased efficiency and affinity of membrane transporters (33).  
168 Under such conditions, bacteria may increasingly rely on substrates whose uptake shows lower  
169 dependence on temperature. In sea-ice brines where less CO<sub>2</sub> is dissolved (34), elevated pH  
170 promotes the conversion of ammonium to ammonia, which diffuses directly into cells without  
171 the aid of transporters in the membrane. Accordingly, species of bacteria and microalgae show a  
172 greater dependence on ammonium and ammonia at low temperatures and high pH than nitrate

173 (35, 36), thereby reducing reliance on membrane transporters. In SBE-LCA, the potentially  
174 efficient utilization of ammonia made other N acquisition genes dispensable, leading to the  
175 neutral loss of nitrite transporter (*nitM*), whereas glutamine synthetase (*glnA*) and glutamate  
176 synthase (*gltS*) responsible for the utilization of ammonia after its assimilation were conserved  
177 (Fig. 1A).

178 An additional stress to *Prochlorococcus* during Snowball Earths was likely the extremely  
179 oligotrophic condition presented by bacteria refugia (37). Accordingly, SBE-LCA of  
180 *Prochlorococcus* evolved a few metabolic strategies for their survival. The amino sugar N-  
181 acetylglucosamine (GlcNAc) is used by bacteria such as *Corynebacterium glutamicum* as a  
182 carbon, energy, and nitrogen source (38). GlcNAc enters bacteria in the form of GlcNAc-6-  
183 phosphate (GlcNAc-6-P). However, instead of being metabolized, the loss of *nagB* for GlcNAc-  
184 6-P deamination at SBE-LCA suggests that GlcN6P is more likely to be involved in  
185 peptidoglycan (PG) recycling through the cascade catalysis by *GlmM* and *GlmU* (Fig. 1A) to  
186 generate UDP-GlcNAc, which is an essential precursor of cell wall PG and LPS (39). During cell  
187 turnovers, PG is continuously broken down and reused through the PG recycling pathway to  
188 produce new PG, and in some bacteria, PG recycling is critical for their long-term survival when  
189 growth is stalled under nutrient limitation (40). Thus, such a recycling mechanism seems to be  
190 key for the maintenance of cell integrity in SBE-LCA under oligotrophic conditions (25).  
191 Glycine betaine (GB) is known to be a ubiquitous protein-stabilizing osmolyte in bacteria, in  
192 particular cyanobacteria (41). However, genes involved in glycine betaine biosynthesis and  
193 transport were lost at SBE-LCA, including *bsmB* for dimethylglycine N-methyltransferase, *gsmt*  
194 for glycine/sarcosine N-methyltransferase, and *proVWXP* for glycine betaine/proline transport  
195 system (Fig. 1A). Instead, several other organic osmolytes might have been used during the

196 Snowball Earths, as their biosynthetic genes were retained at SBE-LCA. The first examples are  
197 the *ggpS* gene encoding glucosylglycerol phosphate synthase for glucosylglycerol (GG)  
198 synthesis and the *gpgS* encoding glucosyl-phosphoglycerate synthase for glucosylglycerate  
199 (GGA) synthesis (Fig. 1A). Since the biosynthesis of GG and GGA requires less N compared to  
200 that of GB (42, 43), the potential use of GG/GGA instead of GB appeared favorable to SBE-  
201 LCA.

202 Low light intensity during Snowball Earth was another formidable challenge to phototrophs  
203 including *Prochlorococcus*. In the Neoproterozoic, the Sun was still at least 6% dimmer than that  
204 at present (44). Moreover, sea ice, especially when covered with snow, is an effective barrier to  
205 light transmission (45). This is in analogy to the deeper layers of today's polar snow and glacier  
206 ice where irradiation is reduced and photosynthetic organisms and activities are scarcely  
207 detectable (46). *Prochlorococcus* may also need to compete with contemporary eukaryotic algae  
208 for the limited amount of light, because the latter became increasingly abundant during the  
209 Cryogenian glaciations and likely shared the same refugia with bacteria (37, 47). Consequently,  
210 photosynthetic organisms trapped in bacterial refugia or inhabiting waters below ice need to be  
211 physiologically geared to cope with low light. It was proposed that modification of the  
212 photosystem structure enables adaptation to the low light condition (48). We inferred a few  
213 changes in photosystem I and II (PSI/PSII) that occurred in SBE-LCA, including the gain of RC1  
214 subunit PsaM, RC2 subunit PsbY, and an extra copy of the RC2 subunit PsbF, the loss of RC2  
215 protein PsbU, and the replacement of RC2 subunit PsbX (Fig. 1A), but the molecular mechanism  
216 of these changes underlying low light adaptation is poorly understood. We also inferred an  
217 expansion of the *Prochlorococcus* antenna Pcb from two to six copies during the Snowball Earth  
218 (Fig. 1A), which may boost the light-harvesting capacity under low-light conditions (49).

219 Many cyanobacteria have a sophisticated circadian clock, which is essential in controlling  
220 the global diel transcriptional activities of the cells. This circadian oscillator system requires only  
221 three components: KaiA, KaiB, and KaiC (50). While all marine *Synechococcus* possess the  
222 three *kai* genes, most *Prochlorococcus* lack *kaiA* and, as a consequence, their circadian clocks  
223 rather behave like an “hourglass” which is reset every morning (51-53). Our analysis indicated  
224 that *kaiA* was lost at SBE-LCA (Fig. 1A). This is likely due to the prolonged darkness or low  
225 light conditions during the Snowball Earth, rendering the sophisticated circadian clock  
226 dispensable.

227 We argue that the genome reduction and metabolic adaptation events discussed above not  
228 only enabled *Prochlorococcus* to survive the Snowball Earth climate catastrophe, but also shaped  
229 the physiological characters and the biogeographic distribution of their descendants in the  
230 modern ocean. For example, the genome reduction that occurred in the early evolution of  
231 *Prochlorococcus* likely resulted in the reduced cell size and increased surface-to-volume ratio in  
232 their descendants, which may have enhanced their efficiency in nutrient acquisition (54) and  
233 eventually led them to dominate the photosynthetic communities in the most oligotrophic regions  
234 of today’s oceans (2). Likewise, new metabolic strategies that *Prochlorococcus* evolved to  
235 overcome the nutrient stresses during Snowball Earth, such as the recycling of cell wall  
236 components and the use of GG and GGA instead of nitrogen-rich GB as the organic osmolytes,  
237 decreased the nutrient requirements of the descendants’ cells and thus contributed to their  
238 success in the modern oligotrophic nitrogen-limited oceans. On the other hand, modifications of  
239 some important metabolic pathways may also have imposed deleterious effects on  
240 *Prochlorococcus* descendants. For example, whereas the replacement of circadian clock with an  
241 hourglass-like mechanism might have facilitated the ancestral lineage to adapt to the prolonged

242 dim light condition during the Snowball Earth catastrophe, it likely prevents the dispersal of  
243 *Prochlorococcus* to high latitude regions in the modern ocean, where the day length varies  
244 substantially across seasons. Normally, organisms with circadian rhythms deal with these  
245 changes by anticipating the changes of light intensity and promptly regulating cellular processes  
246 such as DNA transcription and recombination via chromosome compaction, a known mechanism  
247 to protect DNA from UV radiation (55, 56). In the absence of the circadian clock, however,  
248 species such as *Prochlorococcus* cannot synchronize the endogenous oscillation with the  
249 environmental cycles and thus are at high risks of cell damages (57).

250

## 251 **Caveats and Concluding Remarks**

252 The relaxed clock model implemented in the present study takes into account the rate  
253 variation among species and allows us to estimate a reliable timeline of *Prochlorococcus*  
254 evolution. On this basis, we link an ancestral phylogenetic branch that supported population  
255 bottlenecks and genome reduction of *Prochlorococcus* to the Neoproterozoic Snowball Earth.  
256 Using ancestral gene gain and loss analysis, we further identify potentially important metabolic  
257 strategies that the Cryogenian *Prochlorococcus* evolved to survive the glacial catastrophe.  
258 Despite these fascinating results, there are important caveats. We postulated that the icehouse  
259 conditions during the Cryogenian were lethal to the ancestral *Prochlorococcus* and thus inducing  
260 population bottlenecks. Apparently, this key assumption derives from our knowledge on the  
261 modern *Prochlorococcus* populations which do not grow below ~10°C, but this physiological  
262 character is not necessarily transmissible to the ancestral population. We also postulated that the  
263 metabolic traits we discussed earlier, which allowed *Prochlorococcus* to survive the lethally low  
264 temperature, extremely oligotrophic condition, and low light intensity, each must have conferred

265 a strong fitness advantage (i.e., large selection coefficient  $s$ ) to the Cryogenian *Prochlorococcus*  
266 population. This is because for populations under powerful genetic drift and thus having small  
267 effective population sizes ( $Ne$ ), which is the case for the Cryogenian *Prochlorococcus*  
268 populations, only those mutants that confer sufficiently large benefits ( $s > 1/Ne$ ) can be promoted  
269 by positive selection (58). While the metabolic traits we discussed fit the geochemical conditions  
270 well, they need additional evidence to support the hypothesis that they were subjected to positive  
271 selection and facilitated *Prochlorococcus* adaptation in those harsh conditions. From the  
272 perspective of the dating methodology, the uncertainty of our analysis largely comes from the  
273 use of calibrations. Molecular clock analysis requires at least one maximum age constraint (59).  
274 However, available cyanobacterial fossils can only serve as the minimum bounds (16), and  
275 therefore our analysis has to rely on the maximum bound provided by the root. We took a  
276 conservative approach by successively increasing the maximum bound of the root from 3,800  
277 Ma to 4,500 Ma, which showed that the posterior age of the ancestral node SBE-LCA increased  
278 only slightly by ~7% (Fig. S2 and Table S1) and thus strengthened our conclusion of the  
279 coincidence between SBE-LCA and Cryogenian Snowball Earth.

280 The Neoproterozoic Snowball Earth hypothesis was proposed decades ago, which claimed  
281 the entire extinction of the photosynthetic organisms (21). In contrast to the original “hard”  
282 version of the hypothesis, a modified “soft” version of the Snowball Earth hypothesis was later  
283 proposed to include the likely persistence of refugia across the Cryogenian Period, which  
284 allowed for the survival of bacterial and simple eukaryotic lineages (60, 61). Survivors of the  
285 Snowball Earth included photosynthetic microorganisms (62, 63), which enabled continuous  
286 primary production across the interval (60, 64). Like other autotrophic organisms at the base of a  
287 food web, the survival of *Prochlorococcus* was likely important in sustaining primary

288 production, heterotrophy, and carbon cycling, as well as broader ecosystem functioning during  
289 the Snowball Earth glaciations (60). On the other hand, the population bottlenecks we learned  
290 from *Prochlorococcus* may not necessarily have occurred in other cooccurring photoautotrophic  
291 lineages. Take *Synechococcus*, which evolutionarily most closely related to *Prochlorococcus*, as  
292 an example. The modern *Synechococcus* have wider geographical distribution than  
293 *Prochlorococcus*, and those inhabiting higher latitude regions are known to be more adaptive to  
294 the lower seawater temperature (65, 66). Moreover, *Synechococcus* harbor more diverse  
295 pigments than *Prochlorococcus*, which allow them to live with a wider range of light niches (67).  
296 These unique traits may increase the survivorship of *Synechococcus* during the Snowball Earths  
297 and thus reduce the chance to detect population bottlenecks, if any, in that difficult time.

298 On the other extreme, a few studies have proposed that microbial communities might have  
299 been only mildly affected by the Snowball Earth climate catastrophe (63, 64). These inferences  
300 were based on the microfossil and biomarker records, which, due to the lack of lineage-  
301 specificity, did not capture the nuances required to reconstruct effects on many ecologically  
302 important lineages as the *Prochlorococcus* studied here. Instead, we find that substantial  
303 disruptions to the Earth system, like the Neoproterozoic Snowball Earth, leave indelible  
304 signatures in microbial genomes, such that these heritable changes allow us to reconstruct  
305 interactions between environmental change and biological evolution deep in Earth's history. By  
306 employing the accelerated genome-wide accumulation of the deleterious type mutations as a  
307 proxy for a rapid decrease in the population size of ancient lineages, we uncovered severe  
308 bottlenecks that shaped the early evolution of *Prochlorococcus* lineages. The precise molecular  
309 clock analyses as well as the ancestral genome reconstruction, furthermore, enabled us to link  
310 dynamics in ancestral population sizes to changes in metabolic potential and adaptation to

311 icehouse climates through natural selection. Collectively, our findings demonstrate how  
312 paleomicrontological approaches can be used to connect large-scale dynamics in the Earth  
313 System to the genomic imprints left on extant microorganisms, which shape their ecological role  
314 and biogeographic distribution in the world today. They also illustrate how *Prochlorococcus*  
315 acted as important “guardians of metabolism” (12), safeguarding photosynthetic metabolic  
316 potential across the Snowball Earth climate catastrophe.

317

## 318 **Materials and Methods**

319 Genomic sequences of Cyanobacteria were downloaded from public databases and manually  
320 annotated (see “Dataset\_1.tbl” in online GitHub repository and Section 1 in Supplemental  
321 Methods). Divergence time of *Prochlorococcus* was estimated with MCMCTree v4.9e (68) on  
322 top of 27 genes (see “Dataset\_2.tbl” in online GitHub repository) previously proposed to be  
323 valuable to date bacterial divergence (69) and *Cyanobacteria* phylogenomic trees. In previous  
324 studies, the LPP (*Leptolyngbya*, *Plectonema*, and *Phormidium*) group of *Cyanobacteria* located  
325 either at the basal of the Microcyanobacteria group (14, 70) or at the basal of the  
326 Macrocyanobacteria group (71, 72). Our analysis showed that this controversy is likely caused  
327 by the inclusion of composition-heterogeneous proteins, and that using composition-  
328 homogeneous proteins led to consistent support for the former hypothesis (Fig. S4; see  
329 “Dataset\_3.tbl” in online GitHub repository and Section 2.2 in Supplemental Methods). Since  
330 molecular dating analysis is known to be intrinsically associated with calibration points (73), we  
331 summarized the calibrations of Cyanobacteria used in previous studies and modified them for our  
332 analyses with caution. Moreover, we proposed a new strategy to use calibrations when non-  
333 oxygenic Cyanobacteria were used as outgroups (Table S1; see Section 2.3 in Supplemental

334 Methods for justification). We further assessed the fitness of different molecular clock models  
335 implemented in MCMCTree by using the package “mcmc3r” v0.3.2, based on which we decided  
336 to use the independent rates model for further molecular clock analyses. For each molecular  
337 clock analysis, the software ran twice with a burn-in of 50,000 and a total of 500,000  
338 generations. The convergence was assessed based on the correlations of posterior mean time of  
339 all ancestral nodes between independent runs (Fig. S5). By implementing statistical tests based  
340 on the “infinite-site” theory (Fig. S3; see Section 2.6 in Supplemental Methods) we were able to  
341 select the most precise estimates of *Prochlorococcus* evolutionary timeline for illustration (Fig.  
342 S6) and further discussion.

343 Evolution of genome content via gene gains and losses was inferred using two independent  
344 methods, AnGST (74) and BadiRate v1.35 (75). The former assumes that the statistically  
345 supported topological differences between a gene tree and the species tree result from  
346 evolutionary events (gene loss, gene duplication, HGT, gene birth, and speciation), and infers  
347 these evolutionary events by reconciling the topological incongruences under a generalized  
348 parsimony framework by achieving a minimum number of the evolutionary events along the  
349 species tree, with penalties of an evolutionary event determined by the genome flux analysis  
350 (74). The latter does not rely on the tree topological incongruence information, but instead uses a  
351 full maximum-likelihood approach to determine the gene family turnover rates that maximize the  
352 probability of observing the gene count patterns provided by the family size table. The BadiRate  
353 analyses were run using nine strategies each with a distinct turnover rate model and a distinct  
354 branch model. The likelihoods of different runs were compared, and three strategies with the  
355 highest likelihood values were used (Fig. S7A). Further, results derived from AnGST (Fig. S7B)  
356 and BadiRate were compared and summarized to determine the common patterns shared by the

357 two software (Fig. S7C), and important functional genes discussed were consistently inferred by  
358 these two methods. As the two methods inferred the qualitatively same pattern of genome size  
359 reduction on the branches leading to SBE-LCA, the number of gene gains and losses derived  
360 from the AnGST analysis was presented.

361 The inference of a potential change of selection efficiency on a given branch was performed  
362 by comparing the genome-wide  $d_R/d_C$  value across single-copy orthologous genes of the branch  
363 to that of the closest sister branch. The  $d_R/d_C$  value was calculated using RCCalculator  
364 (<http://www.geneorder.org/RCCalculator/>; see Section 4 in Supplemental Methods) based on two  
365 independent amino acid classification schemes (Table S2).

366

## 367 **Data Availability**

368 The custom scripts as well as the sequence datasets are available in the online GitHub  
369 repository (<https://github.com/luolab-cuhk/Prochl-SBE>).

370

## 371 **Acknowledgments**

372 We thank Allison Coe, Erik Zinser, and Zackary Johnson for providing the data of  
373 *Prochlorococcus* growth rates, Sishuo Wang, Tianhua Liao and Xiaoyuan Feng for their  
374 suggestions on molecular dating analyses. This work is supported by the National Natural  
375 Science Foundation of China (92051113), the Hong Kong Research Grants Council General  
376 Research Fund (14110820), the Hong Kong Research Grants Council Area of Excellence  
377 Scheme (AoE/M-403/16), HKU FoS funds to SAC, and the Direct Grant of CUHK (4053257  
378 and 3132809).

379

380 **References**

- 381 1. S. J. Biller, P. M. Berube, D. Lindell, S. W. Chisholm, Prochlorococcus: the structure and function  
382 of collective diversity. *Nat Rev Microbiol* **13**, 13 (2015).
- 383 2. Z. I. Johnson *et al.*, Niche partitioning among Prochlorococcus ecotypes along ocean-scale  
384 environmental gradients. *Science (80- )* **311**, 1737-1740 (2006).
- 385 3. N. J. West, D. J. Scanlan, Niche-partitioning of Prochlorococcus populations in a stratified water  
386 column in the eastern North Atlantic Ocean. *Appl Environ Microbiol* **65**, 2585-2591 (1999).
- 387 4. W. R. Hess *et al.*, The photosynthetic apparatus of Prochlorococcus: insights through comparative  
388 genomics. *Photosynth Res* **70**, 53-71 (2001).
- 389 5. L. R. Moore, G. Rocap, S. W. Chisholm, Physiology and molecular phylogeny of coexisting  
390 Prochlorococcus ecotypes. *Nature* **393**, 464 (1998).
- 391 6. B. Batut, C. Knibbe, G. Marais, V. Daubin, Reductive genome evolution at both ends of the bacterial  
392 population size spectrum. *Nat Rev Microbiol* **12**, 841 (2014).
- 393 7. H. Luo, R. Friedman, J. Tang, A. L. Hughes, Genome reduction by deletion of paralogs in the  
394 marine cyanobacterium Prochlorococcus. *Mol Biol Evol* **28**, 2751-2760 (2011).
- 395 8. J. Hu, J. L. Blanchard, Environmental sequence data from the Sargasso Sea reveal that the  
396 characteristics of genome reduction in Prochlorococcus are not a harbinger for an escalation in  
397 genetic drift. *Mol Biol Evol* **26**, 5-13 (2008).
- 398 9. H. Luo, Y. Huang, R. Stepanauskas, J. Tang, Excess of non-conservative amino acid changes in  
399 marine bacterioplankton lineages with reduced genomes. *Nat Microbiol* **2**, 17091 (2017).
- 400 10. E. P. Zuckerkandl, Linus, "Evolutionary divergence and convergence in proteins" in *Evolving genes*  
401 and proteins. (Elsevier, 1965), pp. 97-166.
- 402 11. M. O. Dayhoff, A model of evolutionary change in proteins. *Atlas of protein sequence and structure*  
403 **5**, 89-99 (1972).
- 404 12. P. G. Falkowski, T. Fenchel, E. F. Delong, The microbial engines that drive Earth's biogeochemical  
405 cycles. *Science (80- )* **320**, 1034-1039 (2008).
- 406 13. G. C. Kettler *et al.*, Patterns and implications of gene gain and loss in the evolution of  
407 Prochlorococcus. *PLoS Genet* **3**, e231 (2007).
- 408 14. P. Sánchez-Baracaldo, Origin of marine planktonic cyanobacteria. *Sci Rep* **5**, 17418 (2015).
- 409 15. P. Sánchez-Baracaldo, A. Ridgwell, J. A. Raven, A neoproterozoic transition in the marine nitrogen  
410 cycle. *Curr. Biol.* **24**, 652-657 (2014).
- 411 16. C. R. Marshall, Using the Fossil Record to Evaluate Timetree Timescales. *Front Genet* **10**, 1049  
412 (2019).
- 413 17. S. C. Di Rienzi *et al.*, The human gut and groundwater harbor non-photosynthetic bacteria  
414 belonging to a new candidate phylum sibling to Cyanobacteria. *Elife* **2**, e01102 (2013).
- 415 18. R. M. Soo, J. Hemp, D. H. Parks, W. W. Fischer, P. Hugenholtz, On the origins of oxygenic  
416 photosynthesis and aerobic respiration in Cyanobacteria. *Science (80- )* **355**, 1436-1440 (2017).
- 417 19. S. A. Crowe *et al.*, Atmospheric oxygenation three billion years ago. *Nature* **501**, 535 (2013).
- 418 20. N. J. Planavsky *et al.*, Evidence for oxygenic photosynthesis half a billion years before the Great  
419 Oxidation Event. *Nat Geosci* **7**, 283 (2014).
- 420 21. P. F. Hoffman, A. J. Kaufman, G. P. Halverson, D. P. Schrag, A Neoproterozoic snowball earth.  
421 *Science (80- )* **281**, 1342-1346 (1998).
- 422 22. Y. Ashkenazy *et al.*, Dynamics of a Snowball Earth ocean. *Nature* **495**, 90 (2013).
- 423 23. E. R. Zinser *et al.*, Influence of light and temperature on Prochlorococcus ecotype distributions in  
424 the Atlantic Ocean. *Limnol Oceanogr* **52**, 2205-2220 (2007).
- 425 24. D. Thomas, G. Dieckmann, Antarctic sea ice--a habitat for extremophiles. *Science (80- )* **295**, 641-  
426 644 (2002).
- 427 25. P. F. Hoffman *et al.*, Snowball Earth climate dynamics and Cryogenian geology-geobiology. *Sci  
428 Adv* **3**, e1600983 (2017).

429 26. N. Takeuchi, Optical characteristics of cryoconite (surface dust) on glaciers: the relationship  
430 between light absorbency and the property of organic matter contained in the cryoconite. *Annals of*  
431 *Glaciology* **34**, 409-414 (2002).

432 27. F. C. Benforte *et al.*, Novel role of the LPS core glycosyltransferase WapH for cold adaptation in  
433 the Antarctic bacterium *Pseudomonas extremoaustralis*. *PLoS One* **13**, e0192559 (2018).

434 28. Z. Wang, J. Wang, G. Ren, Y. Li, X. Wang, Influence of core oligosaccharide of lipopolysaccharide  
435 to outer membrane behavior of *Escherichia coli*. *Mar Drugs* **13**, 3325-3339 (2015).

436 29. G. Feller, C. Gerdy, Psychrophilic enzymes: hot topics in cold adaptation. *Nat Rev Microbiol* **1**,  
437 200 (2003).

438 30. W. Schumann, Regulation of bacterial heat shock stimulons. *Cell Stress and Chaperones* **21**, 959-  
439 968 (2016).

440 31. A. La Terza, G. Papa, C. Miceli, P. Luporini, Divergence between two Antarctic species of the  
441 ciliate *Euplotes*, *E. focialii* and *E. nobilii*, in the expression of heat-shock protein 70 genes. *Mol*  
442 *Ecol* **10**, 1061-1067 (2001).

443 32. J. P. Rinehart *et al.*, Continuous up-regulation of heat shock proteins in larvae, but not adults, of a  
444 polar insect. *Proc Natl Acad Sci U S A* **103**, 14223-14227 (2006).

445 33. R. P. Lawrence, J. W. William, Temperature and substrates as interactive limiting factors for marine  
446 heterotrophic bacteria. *Aquat. Microb. Ecol.* **23**, 187-204 (2001).

447 34. M. Gleitz, M. R. v.d. Loeff, D. N. Thomas, G. S. Dieckmann, F. J. Millero, Comparison of summer  
448 and winter inorganic carbon, oxygen and nutrient concentrations in Antarctic sea ice brine. *Mar*  
449 *Chem* **51**, 81-91 (1995).

450 35. D. S. Reay, D. B. Nedwell, J. Priddle, J. C. Ellis-Evans, Temperature dependence of inorganic  
451 nitrogen uptake: reduced affinity for nitrate at suboptimal temperatures in both algae and bacteria.  
452 *Appl. Environ. Microbiol.* **65**, 2577-2584 (1999).

453 36. J. A. Raven, B. Wollenweber, L. L. Handley, A comparison of ammonium and nitrate as nitrogen  
454 sources for photolithotrophs. *New Phytol.* **121**, 19-32 (1992).

455 37. P. Hoffman, Cryoconite pans on Snowball Earth: supraglacial oases for Cryogenian eukaryotes?  
456 *Geobiology* **14**, 531-542 (2016).

457 38. A. Uhde *et al.*, Glucosamine as carbon source for amino acid-producing *Corynebacterium*  
458 *glutamicum*. *Appl Microbiol Biotechnol* **97**, 1679-1687 (2013).

459 39. J. T. Park, T. Uehara, How Bacteria Consume Their Own Exoskeletons (Turnover and Recycling  
460 of Cell Wall Peptidoglycan). *Microbiol. Mol. Biol. Rev.* **72**, 211-227 (2008).

461 40. M. Borisova *et al.*, Peptidoglycan Recycling in Gram-Positive Bacteria Is Crucial for Survival in  
462 Stationary Phase. *MBio* **7** (2016).

463 41. G. C. Papageorgiou, N. Murata, The unusually strong stabilizing effects of glycine betaine on the  
464 structure and function of the oxygen-evolving Photosystem II complex. *Photosynth Res* **44**, 243-  
465 252 (1995).

466 42. D. J. Scanlan *et al.*, Ecological genomics of marine picocyanobacteria. *Microbiol. Mol. Biol. Rev.*  
467 **73**, 249-299 (2009).

468 43. N. Empadinhas, M. S. da Costa, To be or not to be a compatible solute: bioversatility of  
469 mannosylglycerate and glucosylglycerate. *Syst Appl Microbiol* **31**, 159-168 (2008).

470 44. J. H. Carver, I. M. Vardavas, Precambrian glaciations and the evolution of the atmosphere. *Ann*  
471 *Geophys* **12**, 674-682 (1994).

472 45. J. A. Raven, J. Kübler, J. Beardall, Put out the light, and then put out the light. *J. Mar. Biol. Assoc.*  
473 *U.K.* **80**, 1-25 (2000).

474 46. C. Simon, A. Wiezer, A. W. Strittmatter, R. Daniel, Phylogenetic diversity and metabolic potential  
475 revealed in a glacier ice metagenome. *Appl Environ Microbiol* **75**, 7519-7526 (2009).

476 47. J. J. Brocks *et al.*, The rise of algae in Cryogenian oceans and the emergence of animals. *Nature*  
477 **548**, 578 (2017).

478 48. R. Kouřil, E. Wientjes, J. B. Bultema, R. Croce, E. J. Boekema, High-light vs. low-light: effect of

479 light acclimation on photosystem II composition and organization in *Arabidopsis thaliana*.  
480 *Biochimica et Biophysica Acta (BBA)-Bioenergetics* **1827**, 411-419 (2013).

481 49. T. Bibby, I. Mary, J. Nield, F. Partensky, J. Barber, Low-light-adapted Prochlorococcus species  
482 possess specific antennae for each photosystem. *Nature* **424**, 1051 (2003).

483 50. G. Dong, S. S. Golden, How a cyanobacterium tells time. *Curr Opin Microbiol* **11**, 541-546 (2008).

484 51. J. Holtzendorff *et al.*, Genome streamlining results in loss of robustness of the circadian clock in  
485 the marine cyanobacterium *Prochlorococcus marinus* PCC 9511. *J Biol Rhythms* **23**, 187-199  
486 (2008).

487 52. I. M. Axmann *et al.*, Biochemical evidence for a timing mechanism in prochlorococcus. *J Bacteriol*  
488 **191**, 5342-5347 (2009).

489 53. D. Mella-Flores *et al.*, *Prochlorococcus* and *Synechococcus* have Evolved Different Adaptive  
490 Mechanisms to Cope with Light and UV Stress. *Front Microbiol* **3**, 285 (2012).

491 54. S. J. Giovannoni, J. C. Thrash, B. Temperton, Implications of streamlining theory for microbial  
492 ecology. *ISME J* **8**, 1553 (2014).

493 55. R. L. Warters, B. W. Lyons, Variation in radiation-induced formation of DNA double-strand breaks  
494 as a function of chromatin structure. *Radiat Res* **130**, 309-318 (1992).

495 56. M. J. Simons, The evolution of the cyanobacterial posttranslational clock from a primitive  
496 “phoscillator”. *J Biol Rhythms* **24**, 175-182 (2009).

497 57. C. W. Mullineaux, R. Stanewsky, The rolex and the hourglass: a simplified circadian clock in  
498 *Prochlorococcus*? *J Bacteriol* **191**, 5333-5335 (2009).

499 58. H. Luo, M. A. Moran, How do divergent ecological strategies emerge among marine  
500 bacterioplankton lineages? *Trends Microbiol* **23**, 577-584 (2015).

501 59. G. J. Szollosi *et al.*, Relative time constraints improve molecular dating. *bioRxiv* (2020).

502 60. M. Moczydłowska, The Ediacaran microbiota and the survival of Snowball Earth conditions.  
503 *Precambrian Res* **167**, 1-15 (2008).

504 61. P. F. Hoffman, D. P. Schrag, The snowball Earth hypothesis: testing the limits of global change.  
505 *Terra nova* **14**, 129-155 (2002).

506 62. C. W. Allison, S. M. Awramik, Organic-walled microfossils from earliest Cambrian or latest  
507 Proterozoic Tindir Group rocks, northwest Canada. *Precambrian Res* **43**, 253-294 (1989).

508 63. F. A. Corsetti, S. M. Awramik, D. Pierce, A complex microbiota from snowball Earth times:  
509 microfossils from the Neoproterozoic Kingston Peak Formation, Death Valley, USA. *Proc Natl  
510 Acad Sci USA* **100**, 4399-4404 (2003).

511 64. A. N. Olcott, A. L. Sessions, F. A. Corsetti, A. J. Kaufman, T. F. De Oliviera, Biomarker evidence  
512 for photosynthesis during Neoproterozoic glaciation. *Science (80- )* **310**, 471-474 (2005).

513 65. P. Flombaum *et al.*, Present and future global distributions of the marine Cyanobacteria  
514 *Prochlorococcus* and *Synechococcus*. *Proc Natl Acad Sci USA* **110**, 9824-9829 (2013).

515 66. K. Zwirglmaier *et al.*, Global phylogeography of marine *Synechococcus* and *Prochlorococcus*  
516 reveals a distinct partitioning of lineages among oceanic biomes. *Environ Microbiol* **10**, 147-161  
517 (2008).

518 67. C. Six *et al.*, Diversity and evolution of phycobilisomes in marine *Synechococcus* spp.: a  
519 comparative genomics study. *Genome Biol* **8**, R259 (2007).

520 68. Z. Yang, PAML 4: phylogenetic analysis by maximum likelihood. *Mol Biol Evol* **24**, 1586-1591  
521 (2007).

522 69. F. U. Battistuzzi, S. B. Hedges, A major clade of prokaryotes with ancient adaptations to life on  
523 land. *Mol Biol Evol* **26**, 335-343 (2008).

524 70. P. M. Shih *et al.*, Improving the coverage of the cyanobacterial phylum using diversity-driven  
525 genome sequencing. *Proc Natl Acad Sci USA* **110**, 1053-1058 (2013).

526 71. C. Blank, P. Sanchez-Baracaldo, Timing of morphological and ecological innovations in the  
527 cyanobacteria—a key to understanding the rise in atmospheric oxygen. *Geobiology* **8**, 1-23 (2010).

528 72. J. C. Uyeda, L. J. Harmon, C. E. Blank, A comprehensive study of cyanobacterial morphological

529 and ecological evolutionary dynamics through deep geologic time. *PLoS One* **11**, e0162539 (2016).

530 73. B. E. Schirrmeyer, P. Sanchez-Baracaldo, D. Wacey, Cyanobacterial evolution during the  
531 Precambrian. *Int J Astrobiol* **15**, 187-204 (2016).

532 74. L. A. David, E. J. Alm, Rapid evolutionary innovation during an Archaean genetic expansion.  
533 *Nature* **469**, 93 (2011).

534 75. P. Librado, F. Vieira, J. Rozas, BadiRate: estimating family turnover rates by likelihood-based  
535 methods. *Bioinformatics* **28**, 279-281 (2011).

536

Fig. 1

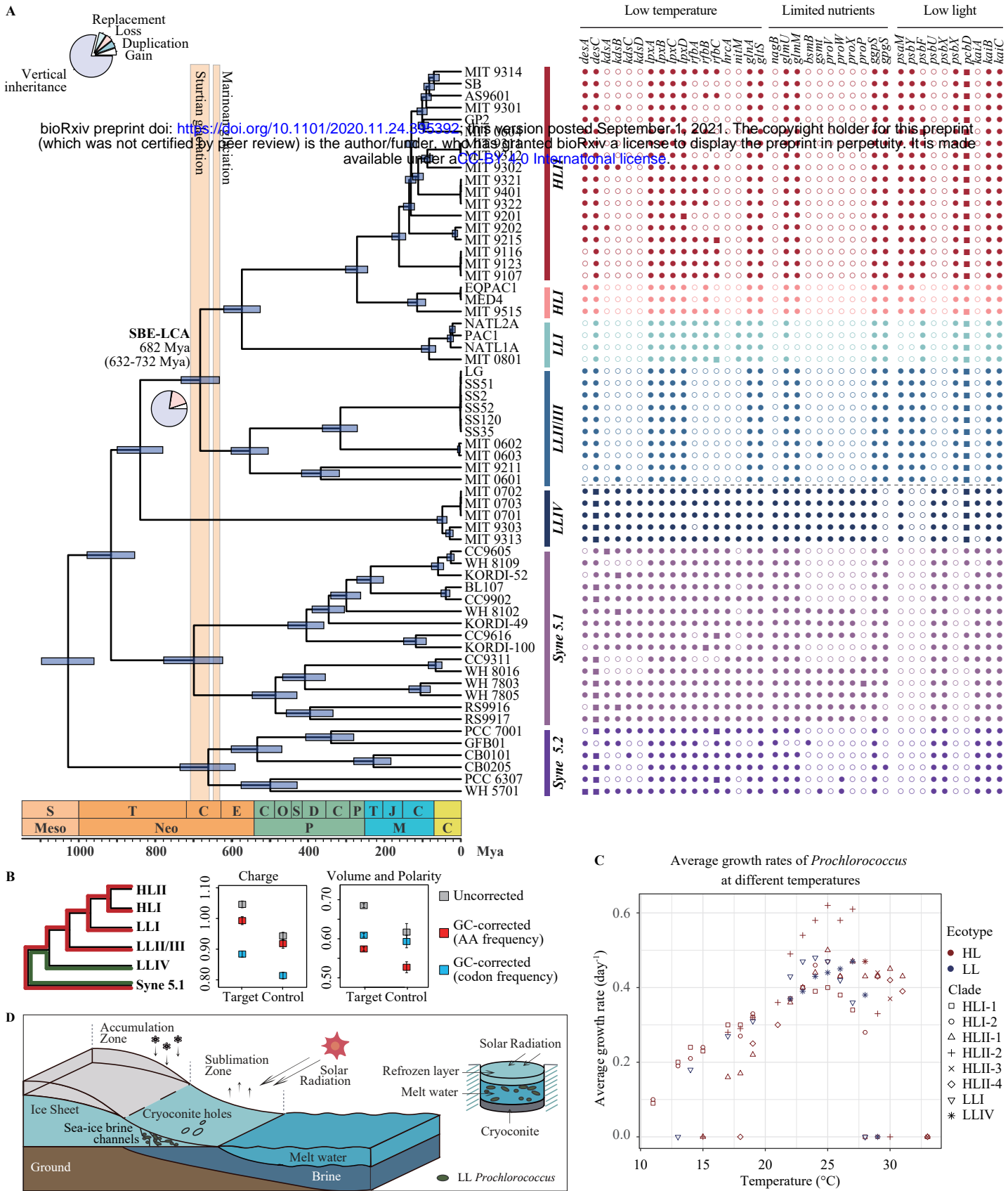


Fig. 1 Evolution of *Prochlorococcus* during the Neoproterozoic Snowball Earth events. (A) (Left) Chronogram of the evolutionary history of *Prochlorococcus* estimated by MCMCTree. The evolutionary tree shown here is part of the species tree constructed with MrBayes based on 90 compositionally homogenous gene families shared by 159 cyanobacterial genomes (Fig. S4 D). Divergence time is estimated based on 27 gene sequences under calibration set C14 (Table S1). The vertical bars represent the estimated time of the Neoproterozoic glaciation events. The flanking horizontal blue bars on ancestral nodes represent the posterior 95% highest probability density (HPD) interval of the estimated divergence time. The pie chart on the ancestral branches leading to the node SBE-LCA provides the proportion of reconstructed genomic events including gene gain, gene loss, gene replacement, gene duplication and gene vertical inheritance. (Right) Phylogenetic pattern of key gene families that potentially enabled *Prochlorococcus* to survive harsh conditions during the Neoproterozoic Snowball Earth (at the ancestral node 'SBE-LCA'). Solid square, solid circle and open circle next to each extant taxon represent multi-copy gene family, single-copy gene family, and absence of the gene family, respectively, in the genome. (B) (Left) The diagram helps understand how the  $d_R/d_C$  was calculated. In this context, the 'Target' group includes all genomes of all HL clades, LLI and LLII/III, the 'Control' group includes all genomes of LLIV, and the 'reference' group includes all genomes of Syne 5.1. The  $d_R/d_C$  for the 'Target' group (shown in Middle & Right) is calculated by comparing a genome from the 'Target' group to a genome from the 'reference' group (marked with red), followed by averaging the value across all possible genome pairs. Likewise, the  $d_R/d_C$  for the 'Control' group (shown in Middle & Right) is calculated by comparing a genome from the 'Control' group to a genome from the 'reference' group (marked with green) and then by averaging the value across all possible genome pairs. (Middle & Right) The genome-wide means of  $d_R/d_C$  values at the ancestral branch leading to SBE-LCA and that at its sister lineage. They were classified based on the physicochemical classification of the amino acids by charge or by volume and polarity, and were either GC-corrected by codon frequency (blue), GC-corrected by amino acid (AA) frequency (red) or uncorrected (gray). Error bars of  $d_R/d_C$  values represent the standard error of the mean. (C) The average growth rate of *Prochlorococcus* ecotypes at different temperatures. Replicate cell cultures were grown in a 14:10 light: dark cycle at  $66 \pm 1 \mu\text{mol m}^{-2}\text{s}^{-1}$ . The growth data used for plotting are collected from Johnson et al. 2006 and Zinser et al. 2007. (D) Diagram of putative bacterial refugia including cryoconite holes and sea ice brine channels in Neoproterozoic Snowball Earth.